


DeepFlood: A deep learning based flood detection framework using feature-level fusion of multi-sensor remote sensing images


A. Emily Jenifer

(School of Computing,
SASTRA University,
Thanjavur, Tamilnadu, India

 <https://orcid.org/0000-0002-5469-1412>, emilyjenifer@sastra.ac.in)

Sudha Natarajan

(School of Computing,
SASTRA University,
Thanjavur, Tamilnadu, India

 <https://orcid.org/0000-0003-1729-6699>, sudha@cse.sastra.edu)

Abstract: Flooding is the most common natural disaster in many countries. Remote sensing images are very much useful in disaster monitoring. The different image modalities from different satellites provide varied information about the earth. The synergistic use of optical and radar data helps in precise flood detection. The central focus of this paper is to identify the flooded regions using a dual patch-based Fully Convolutional Network (FCN) for performing deep learning-based feature fusion. The learned features of FCNs trained independently with Synthetic Aperture Radar (SAR) and Multispectral (MS) images are concatenated to represent the flooding better. A random forest classifier is employed to identify the flood from the fused features. The information retrieved is very much valuable in undertaking necessary rescue efforts in flood-affected areas. The proposed network shows superior performance in flood detection on the images from the SEN12-FLOOD dataset with an accuracy as high as 94.17%.

Keywords: flood detection, synthetic aperture radar, multispectral, convolutional neural network, deep learning.

Categories: I.2.6, I.2.10, I.4.9, I.5.4

DOI: 10.3897/jucs.80734

1 Introduction

Flood is one of the natural disasters that affects the humanity to a greater extent. Both tropical and temperate regions are most commonly affected by floods. They damage crops and property, and also cause loss of human life [Brivio et al. 2002]. Therefore, it is necessary to obtain immediate information of the flood-affected area. Remote sensing has become a very suitable technique to detect flooding without having any direct contact with the land area. The open-access availability of multi-temporal and multi-sensor data makes remote sensing efficient in flood monitoring [Chawan et al. 2020]. The active sensors like (e.g. Sentinel-1) operating in the microwave region and the passive sensors (e.g. Sentinel-2) operating in the infrared and visible regions of the electromagnetic spectrum provide all important information of flood-affected areas [Sanyal and Lu 2004].

The development of satellites with different types of sensors makes us possible to collect multi-modal data in real-time. Thus, the shortfall of single sensor information could be supplemented with another sensor's information [Seo et al. 2018]. Data fusion is an effective technique that combines data from multiple sources to generate high-quality information [Zhang 2010].

Initially, flood detection techniques were limited to aerial images. With the advent of satellite technology, SAR and optical images came into existence [Nazir et al. 2014]. Sentinel-1 (S1) satellite is equipped with SAR active sensor operating in C-band with 5-20m resolution [Geudtner et al. 2014]. It acquires the dual-polarized (Vertical-Vertical (VV) and Vertical-Horizontal (VH)) images of earth with the help of microwaves. SAR is a reliable data acquisition technique during monsoon and high cloud cover because it penetrates cloud and dust [Ban et al. 2010]. The signal depends upon the property of the incoming wave, roughness and dielectric property of the earth surface [Woodhouse 2017]. Smooth surface like water tend to exhibit specular reflection, thereby appears darker in the produced SAR image [Landuyt et al. 2020]. The Multispectral (MS) images consist of various bands with different wavelengths. The Sentinel-2 (S2) satellite is a medium to high resolution (10-60 m) satellite that acquires MS images with 11 spectral bands [Notti et al. 2018]. The natural colour band combination is red (band 4), green (band 3) and blue (band 2). This band combination gives the equivalent images of how our eyes see. Thus water appears in a shade of blue [Du et al. 2016]. The European Space Agency (ESA) has launched these S1 and S2 satellites, which has good global coverage for remotely sensed images [Bangira et al. 2019]. Both S1 and S2 sensor images are freely available from geo data portals like United States Geological Survey (USGS) Earth Explorer [USGS] and Alaska Satellite Facility Distributed Active Archive Centre (ASF DAAC) [ASF].

As far as flood detection is concerned, methods such as visual interpretation [Chambenoit et al. 2003], segmentation using fuzzy logic [Giordano et al. 2005], thresholding [Moser and Serpico 2006], chromatic and textural analysis [Zhao et al. 2011] and Normalized Difference Water Index (NDWI) [Soltanian et al. 2019] were used. These traditional methods have limitations in performance for detecting the flood in complex environment [Hu et al. 2020]. Machine learning (ML) algorithms helped to overcome this weakness. Algorithms such as K-Nearest Neighbour (KNN) [Shahabi et al. 2020], artificial neural network (ANN) [Kia et al. 2021], logistic regression [Tien Bui et al. 2019, Pradhan 2010] and decision tree [Chen et al. 2020a] were applied. However, the ML methods are time-consuming and feature-dependent [Mosavi et al. 2020]. Therefore with the emergence of deep learning (DL) technology, the abundant remote sensing data can be processed to learn the task-relevant features efficiently [Zhang et al. 2016].

In this paper, we design a dual patch Fully Convolutional Network (FCN) architecture for processing the SAR and multispectral images separately. A feature-level fusion followed by a random forest classifier is applied to detect the flood more accurately. The entire methodology is called DeepFlood. The main contributions in this paper are

- I. Fully convolutional neural networks are designed for extracting the features from the patches of SAR and multispectral images.
- II. Feature-level fusion is applied and the flood is detected from the fused features using a random forest classifier.
- III. The proposed DeepFlood architecture is evaluated using bi-temporal images from the SEN12-FLOOD dataset.

The remainder of this paper is organized as follows. The next section presents a brief review of the related work. Section 3 describes the proposed DeepFlood. Section 4 gives the details of the dataset, experiments performed, and results of flood detection. The comparison with the existing approaches in SAR and multispectral based flood detection is given in Section 5.

2 Related work in flood detection

As deep learning and its fusion frameworks have gained importance in recent years [Muñoz et al. 2021], it has been applied to remote sensing extensively. Various SAR and MS-based deep learning approaches for flood detection are discussed in this section.

2.1 SAR-based methods

Due to specular reflection of SAR signals, water surface appears dark in the radar data [Martinis and Rieke 2015]. This property of SAR facilitates in identifying the flooded region. The authors in [Bonafilia et al. 2020] presented a SAR-based flood detection dataset, namely SEN1Floods11, to train and test deep learning models. A fully convolutional neural network was employed to map the flood effectively. In another work [Katiyar et al. 2021], segmentation architectures such as SegNet and UNet were used to improve flood mapping. The authors applied transfer learning for precisely detecting the flooded regions in Kerala, India. Mapping the flood in open area is easier than urban flood mapping due to complex scattering behaviour of urban structures. The work in [Li et al. 2019] introduced an active self-learning convolution neural network framework to map flooding in Houston, USA after a hurricane. Flood mapping with auxiliary hydrological data such as digital elevation model and rainfall information from the meteorology department using VGG16 deep learning network was performed in [Kang et al. 2018].

Flood occurrence is associated with large cloud cover. SAR is capable of penetrating clouds and it is suitable for acquisition in any weather conditions [Dwivedi et al. 2000]. However, the multiplicative noise in SAR makes it difficult to interpret the data effectively [Yu et al. 2018]. This is overcome by fusing images from other sensors such as Sentinel-2.

2.2 Multispectral-based methods

Among all bands of multispectral data, high spatial resolution bands (such as bands 3 to 15) provide supplementary information in flood mapping. These MS band images along with SAR data were used for enhanced flood mapping [Quan et al. 2020]. In [Peng et al. 2019], a patch similarity convolutional neural network was developed for urban flood mapping with spectral reflectance as input to the network. The significance of this deep learning framework is that it does not require any handcrafted flood-related features for training. In order to map flooding in congested areas, a global spatial-spectral convolutional neural network (GSSC) was proposed [Chen et al. 2020b] to extract the water information from MS images effectively. Though the study paves the way to fuse bi-temporal remote sensing images, the single sensor MS images have an impact on the accuracy of the flood mapping due to the presence of clouds. In another work [Wieland et al. 2019a], rapid segmentation of flooded areas on MS images was done with convolutional neural network for situational awareness in emergency response. Although

this study focuses on urban flood detection, the polarimetry information from other sensors in addition can improve the results. Semantic water segmentation is effectively done with the CNN (U-Net) [Wieland et al. 2019b], and the results show a good accuracy of 92%. Most of the flood scenes have challenges in processing due to the presence of clouds and shadows. These challenges can be addressed by augmenting the MS data with other sensor information.

To inherit the advantages of different sensors in terms of spatial and spectral characteristics and to improve flood mapping for precisely assessing the damage, multi-sensor image fusion is considered in this paper. We use the feature-level fusion of multispectral and SAR images for identifying the flood. *To our knowledge, there is no work exclusively on deep learning-based image fusion to identify the flood in the images of SEN12-FLOOD dataset.*

3 Proposed DeepFlood architecture

The proposed DeepFlood architecture for flood detection consists of dual patch Fully Convolutional Network (FCN) for feature extraction, followed by a feature fusion and a random forest classifier, as shown in Figure 1. The two patch FCNs are separately trained with SAR and multispectral images. A feature-level fusion is performed to concatenate the learned features of SAR and MS. Then, a random forest classifier [Leo 2001] is used to classify the *Flood* and *No Flood* patches. In order to classify the entire image of a region, maximum vote of patch classes is considered. The different stages of DeepFlood architecture are explained in detail next.

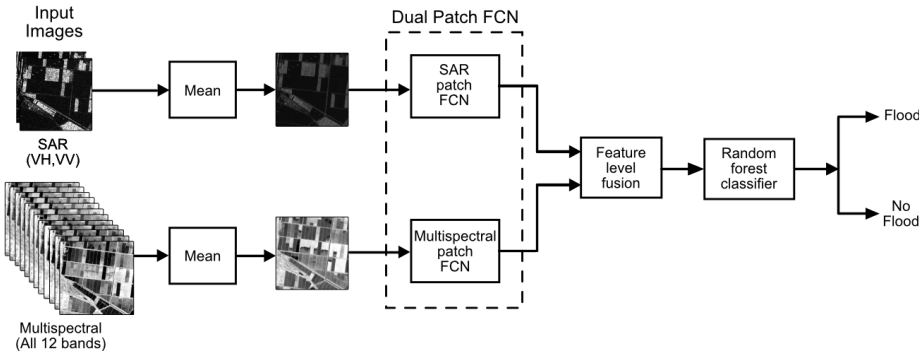


Figure 1: Proposed DeepFlood architecture

3.1 Dual patch FCN for feature extraction

The proposed dual patch FCN (Figure 2) consists of two 10-layered identical fully convolutional networks. One FCN processes 75×75 SAR image patches, and the other processes 75×75 MS image patches. The inputs of sizes $75 \times 75 \times 2$ of SAR and $75 \times 75 \times 11$ of multispectral are given separately to two FCNs. A sequence of 5 pairs of

convolution and max-pooling layers processes these patches. Each convolution layer uses a filter kernel of size 3×3 for learning the features and each max-pooling layer considers blocks of size 2×2 for dimensionality reduction. The convolutions are performed with zero padding and stride 2. The number of filters is doubled at each layer to increase the number of feature maps. The first convolutional layer has 64 filters of size 3×3 . The second convolutional layer has 128 filters of size 3×3 . The remaining three layers have 128, 256 and 512 filters each of size 3×3 . Further, regularization techniques like batch normalization and dropouts are added to improve the generalization of the network. The independently learned SAR and MS features are flattened and concatenated at last for feature fusion.

For learning the features, the networks are independently trained with their respective images. A fully connected layer is added at the end of each network to train the networks for *Flood* and *No Flood* classification. The fully connected layer has 4608 input units ($3 \times 3 \times 512$). Once the training is over, these fully connected layers are discarded and the convolutional networks are capable of extracting relevant features from the input images.

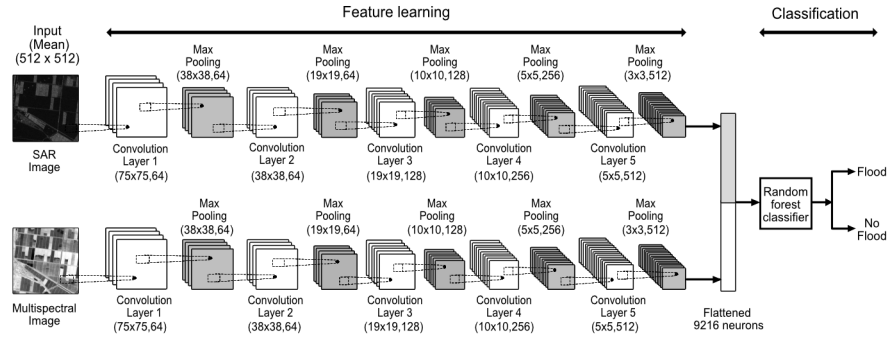


Figure 2: Proposed dual patch FCN

3.2 Feature-level fusion and classification

The feature fusion is applied by concatenating the flattened feature maps of SAR (FM_{sar}) and MS (FM_{ms}) images obtained from the trained dual patch FCN. The fused feature vector (FM_{fus}) contains the needful information from both sensor images for classification.

$$Fusion\ function\ f : \{FM_{sar}, FM_{ms}\} \rightarrow FM_{fus} \quad (1)$$

Finally, the fused features are fed to a random forest classifier for *Flood* and *No Flood* classification. Random forest is an ensemble learning which combines many decision trees classifiers to provide the solution to a complex problem. For the classification problem, the trees in random forest cast their vote [Gislason et al. 2006]. The output class is based on the majority votes of the trees. In the DeepFlood architecture, a random forest classifier with 250 estimators (trees) is added after the FCN for the final classification of *Flood* and *No Flood* images.

4 Experiments and results

The DeepFlood architecture was implemented in Python with TensorFlow library and run on a workstation with 16 GB RAM, Intel Core i7-9700K CPU230 and NVIDIA Titan 3840 XP GPU.

4.1 Dataset

SEN12-FLOOD dataset [Rambour et al. 2020b], available at IEEE data port, was used to evaluate the efficacy of the proposed DeepFlood framework. It is a recently created fairly large dataset for flood detection studies [Rambour et al. 2020a] using deep learning. The dataset consists of pre-flood and post-flood images of 336 flood events in West and South-East Africa, Middle-East countries, and Australia. The images are acquired by the Sentinel 1 and 2 sensors. The Sentinel 1 SAR (with Vertical Vertical - VV and Vertical Horizontal - VH polarization) data were acquired in interferometric wide swath mode with a resolution of 10×10 m and pre-processed for radiometric calibration and range-Doppler terrain correction. The Sentinel 2 multispectral (12 bands) data were pre-processed for Level 2A atmospheric correction. Both the SAR (VV and VH) and multispectral (all 12 bands) images were resized to 512×512 . The mean image of all the bands in the case of multispectral and the mean of VV and VH images in the case of SAR were computed. They were fed as inputs to FCN. The sample post-flood SAR and multispectral images from the SEN12-Flood dataset and their mean images are shown in (Figures 3 and 4)

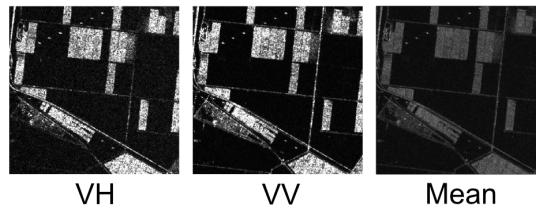


Figure 3: Sample post-flood SAR images

4.2 Dual patch FCN training

The inputs to the dual patch FCN are SAR and MS images patches of size 75×75 . One of the patch FCNs was trained with SAR image patches while the other with multispectral patches. From the SEN12-FLOOD dataset, 480 cloud-free MS images (240 *Flood* and 240 *No Flood*) and their corresponding 480 SAR images were taken for training. The network was trained with K-Fold (K=8) cross-validation. 120 SAR and 120 MS (60 *Flood* and 60 *No Flood*) images were considered for testing. The FCNs were trained with a batch size of 32 and a learning rate of 0.01. RMSprop optimizer was chosen for optimization.

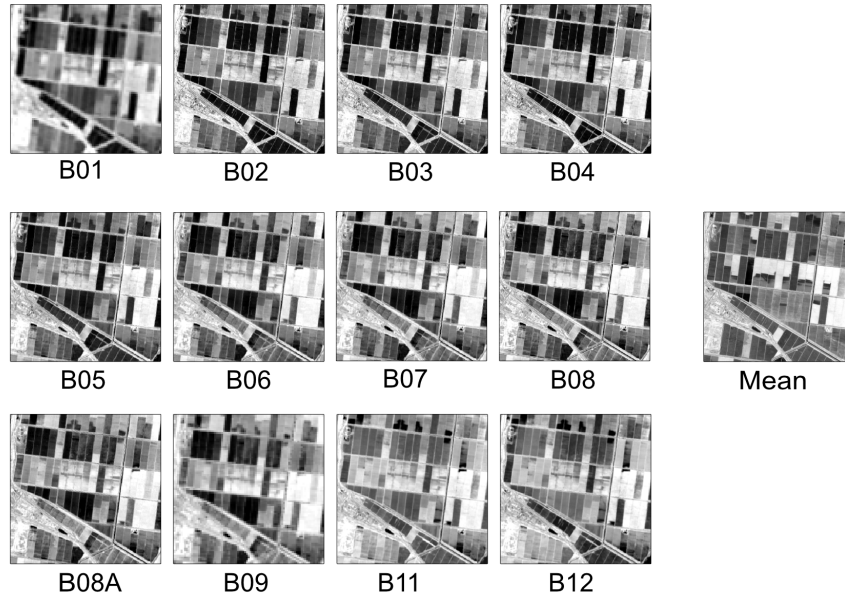


Figure 4: Sample post-flood MS images

4.3 Performance evaluation

The commonly used metrics such as precision, recall, F1-score and classification accuracy derived from the confusion matrix are used to evaluate the classification performance of the proposed DeepFlood architecture. True Positives (TP), False Positives (FP) and False Negatives (FN) are computed for *Flood* and *No Flood* classes. In the case of *Flood* class, TP is the number of *Flood* images that are classified correctly. FN is the number of *Flood* images that are classified as *No Flood*. FP is the number of *No Flood* images that are classified as a *Flood*. Precision (Producer Accuracy-PA) measures the fraction of the identified positives that are true positives and hence in the case of *Flood* class, PA is the fraction of patches classified as *Flood* by the network actually belongs to *Flood*. Recall (User Accuracy-UA) gives the fraction of correctly identified positives. It is the fraction of *Flood* patches that are classified as a *Flood* by the network. F1-score considers both PA and UA. The metrics are computed using TP, FN, FP and TN values.

$$Recall(UA) = \frac{TP}{(TP + FN)} \quad (2)$$

$$Precision(PA) = \frac{TP}{(TP + FP)} \quad (3)$$

$$F1 - score = \frac{2}{\frac{1}{UA} + \frac{1}{PA}} \quad (4)$$

$$Accuracy = \frac{TP + TN}{(TP + TN + FP + FN)} \quad (5)$$

Class	Precision	Recall	F1-Score
Flood	0.83	0.87	0.85
NoFlood	0.86	0.82	0.84

Table 1: Classification performance metrics of SAR patch FCN

For the independently trained SAR and MS networks, the confusion matrices are shown in Figures 5 and 6 respectively. The confusion matrix (fused) giving the classification results of DeepFlood architecture is shown in Figure 7. The metrics computed are listed in Tables 1, 2 and 3. The feature maps generated from the first convolutional layer of SAR and MS-based FCNs are shown in Figure 8. From these results, it can be inferred that the fused network performs better than the independent networks. Further, SAR-based FCN performs better than MS-based FCN because SAR images are more responsive to water pixels than MS images due to their sensitivity to water and moisture. However, the additional spectral features of the MS images contribute to the improved results in DeepFlood architecture. The flood detection results of a region before and after a flood event are shown in Figure 9 on the underlying mean SAR images. The results are given for 75×75 patches of the entire 512×512 image of the region. The patches identified as *Flood* by the DeepFlood architecture are denoted by 'F'. Most of the flooded areas are identified after flooding while in the image of the region before the flood event, no patch is identified as *Flood*.

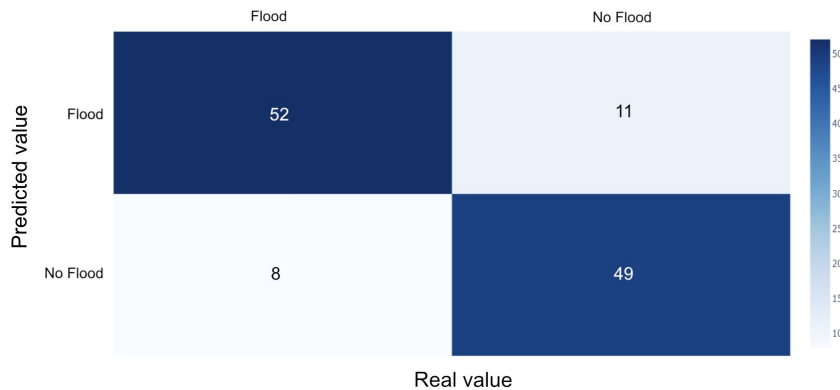


Figure 5: Confusion matrix of SAR patch FCN

4.4 Ablation studies

Ablation studies have been conducted to analyse the performance of random forest classifier. We analysed the classification performance for increasing number of estimators to decide the optimal number. It is observed from Figure 10 that the classification accuracy

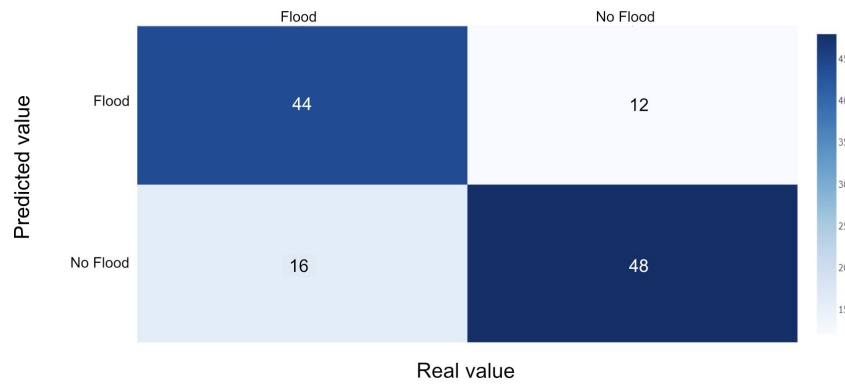


Figure 6: Confusion matrix of MS patch FCN

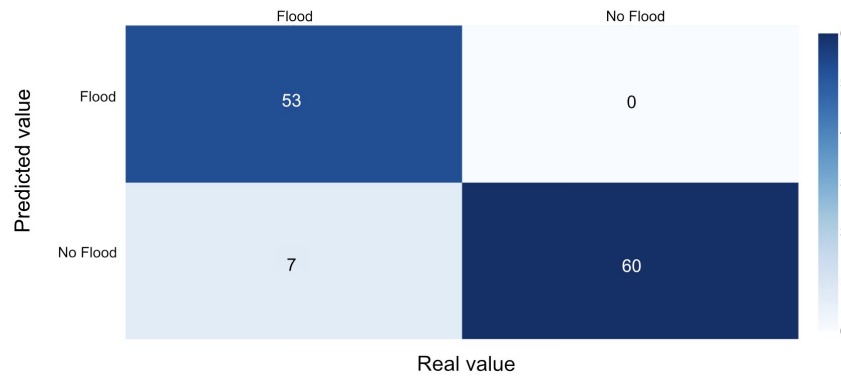


Figure 7: Confusion matrix of DeepFlood with feature fusion

increases up to 250 estimators and then begin to decrease. The number of estimators is therefore fixed to 250.

5 Comparison studies

The recent works that apply the SAR and multispectral images for flood detection were considered for comparison. The results of the proposed DeepFlood architecture and exist-

Class	Precision	Recall	F1-Score
Flood	0.79	0.73	0.76
NoFlood	0.75	0.80	0.77

Table 2: Classification performance metrics of MS patch FCN

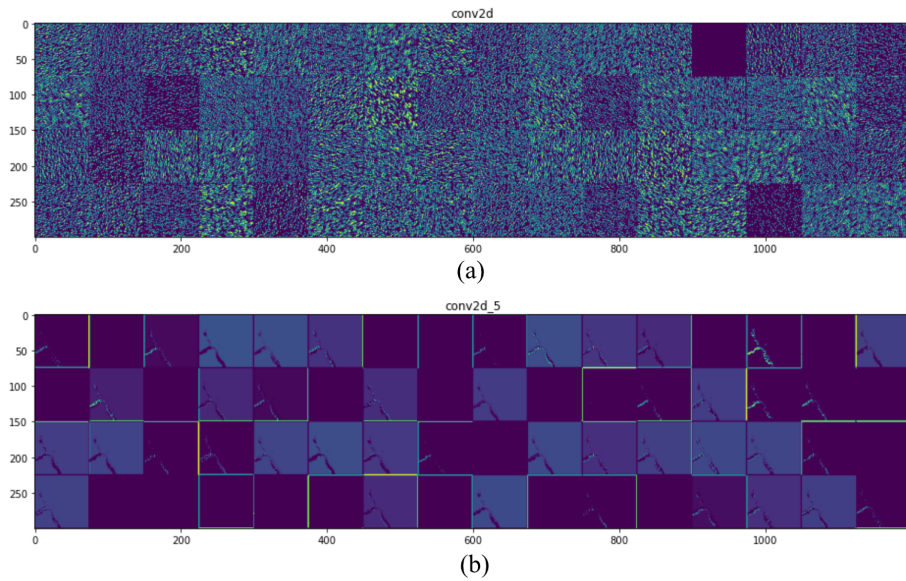


Figure 8: Feature maps from the first convolutional layer of (a) SAR patch FCN (b) MS patch FCN

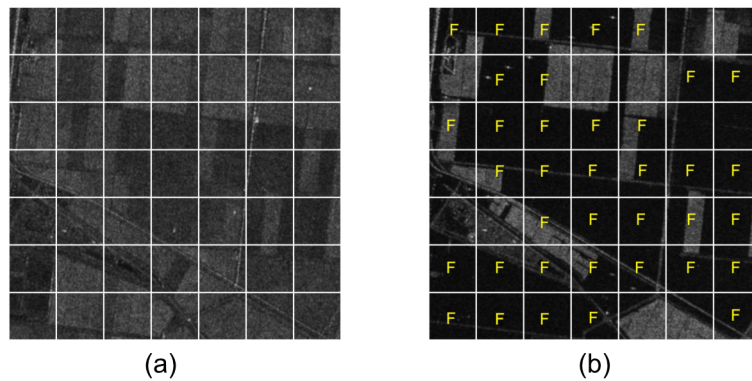


Figure 9: Flood detection (a) Before flood event (b) After flood event

ing flood detection approaches are provided in Table 4. One approach [Jacinth Jennifer et al. 2020] derives Normalized Difference Water Index (NDWI) for detecting flood. It is a statistical method but not very effective in identifying floods in urban areas. In another work, Relevance Vector Machine (RVM) [Sharifi 2020] has been applied on SAR to map flooded areas. Although the flood detection accuracy is reasonably high for SAR alone, taking advantage of another sensor information might help to increase the accuracy. A few deep learning based solutions are available in recent works. A Convolutional Neural Network (CNN) [Bhadra et al. 2020] architecture has been designed for identifying flood from multi-sensor data. It however achieves a lower accuracy due to smaller training

Class	Precision	Recall	F1-Score
Flood	1.00	0.88	0.94
NoFlood	0.90	1.00	0.94

Table 3: Classification performance metrics of DeepFlood

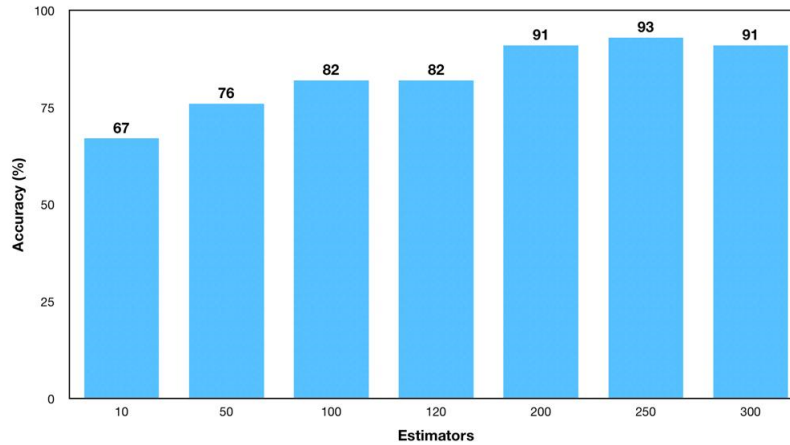


Figure 10: Ablation studies on random forest classifier

and testing datasets (with only 100 and 10 images respectively). On the SEN12-Flood dataset, a RESNET [Rambour et al. 2020a] has been applied independently for SAR and MS. On the same dataset, our proposed DeepFlood architecture gives better flood detection accuracies for both SAR and MS. By taking advantage of the feature fusion, the accuracy is further improved. The proposed fusion architecture gives the best accuracy when compared to other methods.

6 Conclusion

In this paper, a deep learning-based methodology, namely DeepFlood, was developed to perform feature-level fusion for *Flood* and *No Flood* classification of regions from their multisensor images. The multisensory (SAR and multispectral) image patches were initially fed to a dual patch FCN. The dual patch FCN is used for feature extraction and fusion of multi-sensor images. The SAR and multispectral perform differently in identifying the flood features. A suitably designed dual patch-based FCN along with a random forest classifier performs better than existing standard deep networks in flood detection. The proposed DeepFlood framework achieves the best accuracy of 94.17% in classifying the images in SEN12-FLOOD dataset.

Approach	Study area/Dataset	Data	Flood detection accuracy
NDWI [Jacinth Jennifer et al. 2020]	Alappuzha region, Kerala	SAR and MS	83% (SAR+MS)
RVM [Sharifi 2020]	Aqqala, Iran	SAR	89% (SAR)
CNN [Bhadra et al. 2020]	Barpeta and Kamrup of Assam, India	SAR and MS	80% (SAR+MS)
ResNet-50 [Rambour et al. 2020a]	SEN12-FLOOD Dataset	SAR and MS	79% (MS), 75% (SAR)
DeepFlood	SEN12-FLOOD Dataset	SAR and MS	94.17% (SAR+MS), 84.17% (SAR), 76.67% (MS)

Table 4: Comparison study

Acknowledgement

The authors would like to thank the Indian Space Research Organization (ISRO) for supporting this research work via the ISRO RESPOND project ISRO/RES/4/ 685/20-21.

Data and Code Availability

The codes, sample inputs and outputs are available at the GitHub repository <https://github.com/emideepak/DeepFlood>

References

- [Ban et al. 2010] Ban, Y., Hu, H., Rangel, I. M.: “Fusion of Quickbird MS and RADARSAT SAR data for urban land-cover mapping: Object-based and knowledge-based approach”; *International Journal of Remote Sensing*, 31(6), (Mar 2010), 1391-1410.
- [Bangira et al. 2019] Bangira, T., Alfieri, S. M., Menenti, M., Van Niekerk, A.: “Comparing thresholding with machine learning classifiers for mapping complex water”; *Remote Sensing*, 11(11), (Jan 2019), 1351.
- [Bhadra et al. 2020] Bhadra, T., Chouhan, A., Chutia, D., Bhowmick, A., Raju, P. L. N.: “Flood Detection Using Multispectral Images and SAR Data”; In *International Conference on Machine Learning, Image Processing, Network Security and Data Sciences* (pp. 294-303). Springer, Singapore (July 2020).
- [Bonafilia et al. 2020] Bonafilia, D., Tellman, B., Anderson, T., Issenberg, E.: “Sen1Floods11: a georeferenced dataset to train and test deep learning flood algorithms for Sentinel-1”; In *Proceedings of the IEEE/CVF Conference on Computer Vision and Pattern Recognition Workshops* (pp. 210-211), (2020).
- [Brivio et al. 2002] Brivio, P. A., Colombo, R., Maggi, M., Tomasoni, R.: “Integration of remote sensing data and GIS for accurate mapping of flooded areas”; *International Journal of Remote Sensing*, 23(3), (Jan 2002), 429-441.

- [Chambenoit et al. 2003] Chambenoit, Y., Classeau, N., Trouvé, E., Rudant, J. P.: "Performance assessment of multitemporal SAR images' visual interpretation"; In IGARSS 2003. 2003 IEEE International Geoscience and Remote Sensing Symposium. Proceedings (IEEE Cat. No. 03CH37477) (Vol. 6, pp. 3911-3913). IEEE, (July 2003).
- [Chawan et al. 2020] Chawan, A. C., Kakade, V. K., Jadhav, J. K.: "Automatic detection of flood using remote sensing images"; *Journal of Information Technology*, 2(01), (2020), 11-26.
- [Chen et al. 2020a] Chen, W., Li, Y., Xue, W., Shahabi, H., Li, S., Hong, H., Ahmad, B. B.: "Modeling flood susceptibility using data-driven approaches of naïve bayes tree, alternating decision tree, and random forest methods"; *Science of The Total Environment*, 701, (Jan 2020), 134979.
- [Chen et al. 2020b] Chen, Y., Tang, L., Kan, Z., Bilal, M., Li, Q.: "A novel water body extraction neural network (WBE-NN) for optical high-resolution multispectral imagery"; *Journal of Hydrology*, 588, (Sep 2020), 125092.
- [Du et al. 2016] Du, Y., Zhang, Y., Ling, F., Wang, Q., Li, W., Li, X.: "Water bodies' mapping from Sentinel-2 imagery with modified normalized difference water index at 10-m spatial resolution produced by sharpening the SWIR band"; *Remote Sensing*, 8(4), (Apr 2016), 354.
- [Dwivedi et al. 2000] Dwivedi, R. S., Rao, B. R. M., Kushwaha, S. P. S.: "The Utility of Day and Night Observation and Cloud Penetration Capability of ERS 1 SAR Data for Detection of Wetlands"; *Geocarto International*, 15(1), (Mar 2000), 7-12.
- [ASF] ASF U.S. Geological. URL <https://earthdata.nasa.gov/eosdis/daacs/asf/>.
- [Geudtner et al. 2014] Geudtner, D., Torres, R., Snoeij, P., Davidson, M., Rommen, B.: "Sentinel-1 system capabilities and applications"; In 2014 IEEE Geoscience and Remote Sensing Symposium (pp. 1457-1460). IEEE, (July 2014).
- [Giordano et al. 2005] Giordano, F., Goccia, M., Dellepiane, S.: "Segmentation of coherence maps for flood damage assessment, Image Processing"; *ICIP 2005. In IEEE International Conference on*, pp. II-233-6, (2005).
- [Gislason et al. 2006] Gislason, P. O., Benediktsson, J. A., Sveinsson, J. R.: "Random forests for land cover classification"; *Pattern recognition letters*, 27(4), (Mar 2006), 294-300.
- [Hu et al. 2020] Hu, S., Qin, J., Ren, J., Zhao, H., Ren, J., Hong, H.: "Automatic extraction of water inundation areas using Sentinel-1 data for large plain areas"; *Remote Sensing*, 12(2), (Jan 2020), 243.
- [Jacinth Jennifer et al. 2020] Jacinth Jennifer, J., Saravanan, S., Abijith, D.: "Integration of SAR and multi-spectral imagery in flood inundation mapping—a case study on Kerala floods 2018"; *ISH Journal of Hydraulic Engineering*, 1-11, (Jul 2020).
- [Kang et al. 2018] Kang, W., Xiang, Y., Wang, F., Wan, L., You, H.: "Flood detection in gaofen-3 SAR images via fully convolutional networks"; *Sensors*, 18(9), (Sep 2018), 2915.
- [Katiyar et al. 2021] Katiyar, V., Tamkuan, N., Nagai, M.: "Near-Real-Time Flood Mapping Using Off-the-Shelf Models with SAR Imagery and Deep Learning"; *Remote Sensing*, 13(12), (Jan 2021), 2334.
- [Kia et al. 2012] Kia, M. B., Pirasteh, S., Pradhan, B., Mahmud, A. R., Sulaiman, W. N. A., Moradi, A.: "An artificial neural network model for flood simulation using GIS: Johor River Basin, Malaysia"; *Environmental earth sciences*, 67(1), (Sep 2012), 251-264.
- [Landuyt et al. 2020] Landuyt, L., Verhoest, N. E., Van Coillie, F.: "Flood Mapping in Vegetated Areas Using an Unsupervised Clustering Approach on Sentinel-1 and-2 Imagery"; *Remote Sensing*, 12(1), (Jan 2020), 3611.
- [Leo 2001] Breiman, L.: "Random forests"; *Machine learning*, 45, (2001), 5–32.

- [Li et al. 2019] Li, Y., Martinis, S., Wieland, M.: “Urban flood mapping with an active self-learning convolutional neural network based on TerraSAR-X intensity and interferometric coherence”; *ISPRS Journal of Photogrammetry and Remote Sensing*, 152, (Jun 2019), 178-191.
- [Martinis and Rieke 2015] Martinis, S., Rieke, C.: “Backscatter analysis using multi-temporal and multi-frequency SAR data in the context of flood mapping at River Saale, Germany”; *Remote Sensing*, 7(6), (Jun 2015), 7732-7752.
- [Melesse et al. 2011] Melesse, A. M., Ahmad, S., McClain, M. E., Wang, X., Lim, Y. H.: “Suspended sediment load prediction of river systems: An artificial neural network approach”; *Agricultural Water Management*, 98(5), (Mar 2011), 855-866.
- [Mosavi et al. 2020] Mosavi, A., Golshan, M., Janizadeh, S., Choubin, B., Melesse, A. M., Dineva, A. A.: “Ensemble models of GLM, FDA, MARS, and RF for flood and erosion susceptibility mapping: a priority assessment of sub-basins”; *Geocarto International*, (Oct 2020), 1-20.
- [Moser and Serpico 2006] Moser, G., Serpico, S. B.: “Generalized minimum-error thresholding for unsupervised change detection from SAR amplitude imagery”; *IEEE Transactions on Geoscience and Remote Sensing*, 44(10), (Sep 2006), 2972-2982.
- [Muñoz et al. 2021] Muñoz, D. F., Muñoz, P., Moftakhari, H., Moradkhani, H.: “From local to regional compound flood mapping with deep learning and data fusion techniques”; *Science of The Total Environment*, 782, (Aug 2021), 146927.
- [Nazir et al. 2014] Nazir, F., Riaz, M. M., Ghafoor, A., Arif, F.: “Flood detection/monitoring using adjustable histogram equalization technique”; *The Scientific World Journal*, (Jan 2014).
- [Notti et al. 2018] Notti, D., Giordan, D., Caló, F., Pepe, A., Zucca, F., Galve, J. P.: “Potential and limitations of open satellite data for flood mapping”; *Remote Sensing*, 10(11), (Nov 2018), 1673.
- [Peng et al. 2019] Peng, B., Meng, Z., Huang, Q., Wang, C.: “Patch similarity convolutional neural network for urban flood extent mapping using bi-temporal satellite multispectral imagery”; *Remote Sensing*, 11(21), (Jan 2019), 2492.
- [Pradhan 2010] Pradhan, B.: “Flood susceptible mapping and risk area delineation using logistic regression, GIS and remote sensing”; *Journal of Spatial Hydrology*, 9(2), (Jan 2010).
- [Quan et al. 2020] Quan, Y., Tong, Y., Feng, W., Dauphin, G., Huang, W., Xing, M.: “A Novel Image Fusion Method of Multi-Spectral and SAR Images for Land Cover Classification”; *Remote Sensing*, 12(22), (Jan 2020), 3801.
- [Rambour et al. 2020a] Rambour, C., Audebert, N., Koeniguer, E., Le Saux, B., Crucianu, M., Datcu, M.: “Flood detection in time series of optical and sar images”; *International Archives of the Photogrammetry, Remote Sensing and Spatial Information Sciences*, 43, (2020), 1343-1346.
- [Rambour et al. 2020b] Rambour, C., Audebert, N., Koeniguer, E., Le Saux, B., Crucianu, M., Datcu, M.: “SEN12-FLOOD : a SAR and Multispectral Dataset for Flood Detection”; *IEEE Dataport*. <https://dx.doi.org/10.21227/w6xz-s898>, (2020).
- [Sanyal and Lu 2004] Sanyal, J., Lu, X. X.: “Application of remote sensing in flood management with special reference to monsoon Asia: a review”; *Natural Hazards*, 33(2), (Oct 2004), 283-301.
- [Seo et al. 2018] Seo, D. K., Kim, Y. H., Eo, Y. D., Lee, M. H., Park, W. Y.: “Fusion of SAR and multispectral images using random forest regression for change detection”; *ISPRS International Journal of Geo-Information*, 7(10), (Oct 2018), 401.
- [Shahabi et al. 2020] Shahabi, H., Shirzadi, A., Ghaderi, K., Omidvar, E., Al-Ansari, N., Clague, J. J., Ahmad, A.: “Flood detection and susceptibility mapping using sentinel-1 remote sensing data and a machine learning approach: Hybrid intelligence of bagging ensemble based on k-nearest neighbor classifier”; *Remote Sensing*, 12(2), (Jan 2020), 266.

- [Sharifi 2020] Sharifi, A.: "Flood mapping using relevance vector machine and SAR data: A case study from Aqqala, Iran"; *Journal of the Indian Society of Remote Sensing*, 48(9), (Sep 2020), 1289-1296.
- [Soltanian et al. 2019] Soltanian, F. K., Abbasi, M., Bakhtyari, H. R.: "Flood monitoring using Ndw and Mndwi spectral indices: A case study of Aghqala flood-2019, Golestan Province, Iran"; *The International Archives of Photogrammetry, Remote Sensing and Spatial Information Sciences*, 42, 605-607.
- [USGS] USGS U.S. Geological Survey. URL <https://earthexplorer.usgs.gov/>.
- [Tien Bui et al. 2019] Tien Bui, D., Khosravi, K., Shahabi, H., Daggupati, P., Adamowski, J. F., Melesse, A. M., Lee, S.: "Flood spatial modeling in northern Iran using remote sensing and gis: A comparison between evidential belief functions and its ensemble with a multivariate logistic regression model"; *Remote Sensing*, 11(13), (Jan 2019), 1589.
- [Wieland et al. 2019a] Wieland, M., Martinis, S., Li, Y.: "Semantic segmentation of water bodies in multi-spectral satellite images for situational awareness in emergency response"; *The International Archives of Photogrammetry, Remote Sensing and Spatial Information Sciences*, 42, (2019) 273-277.
- [Wieland et al. 2019b] Wieland, M., Martinis, S.: "A modular processing chain for automated flood monitoring from multi-spectral satellite data"; *Remote Sensing*, 11(19), (Jan 2019), 2330.
- [Woodhouse 2017] Iain H Woodhouse. "Introduction to microwave remote sensin";g. CRC press, 2017.
- [Yu et al. 2018] Yu, Z., Wang, W., Li, C., Liu, W., Yang, J.: "Speckle noise suppression in SAR images using a three-step algorithm"; *Sensors*, 18(11), (Nov 2018), 3643.
- [Zhang 2010] Zhang, J.: "Multi-source remote sensing data fusion: status and trends"; *International Journal of Image and Data Fusion*, 1(1), (Mar 2010), 5-24.
- [Zhang et al. 2016] Zhang, L., Xia, G. S., Wu, T., Lin, L., Tai, X. C.: "Deep learning for remote sensing image understanding"; *Journal of Sensors*, (Nov 2016).
- [Zhao et al. 2011] Zhao, M., Shang, H., Huang, W., Zou, L., Zhang, Y.: "Flood area extraction from rgb aerophotograph based on chromatic and textural analysis"; In *International Conference on Advanced Geographic Information Systems, Applications and Services GeoProcessing* (pp. 46-52), (2011).